Electrostatic effect of surfactant molecules on bacteriochlorophyll a and carotenoid binding sites in the LH1 complex isolated from Rhodospirillum rubrum S1 probed by Stark spectro…

ARTICLE *in* PHOTOSYNTHESIS RESEARCH · MARCH 2008

Impact Factor: 3.5 · DOI: 10.1007/s11120-007-9257-y · Source: PubMed

Photosynth Res (2008) 95:345–351
DOI 10.1007/s11120-007-9257-y

REGULAR PAPER

Electrostatic effect of surfactant molecules on bacteriochlorophyll *a* and carotenoid binding sites in the LH1 complex isolated from *Rhodospirillum rubrum* S1 probed by Stark spectroscopy

Katsunori Nakagawa · Satoru Suzuki · Ritsuko Fujii · Alastair T. Gardiner · Richard J. Cogdell · Mamoru Nango · Hideki Hashimoto

Received: 10 September 2007 / Accepted: 10 September 2007 / Published online: 6 October 2007

Abstract The LH1 complexes were isolated from the purple photosynthetic bacterium *Rhodospirillum rubrum* strain S1. They were initially solubilized using LDAO and then purified in the presence of Triton X-100. The purified complexes were then either used directly or following an exchange into LDAO. Stark spectroscopy was applied to probe the electrostatic field around the bacteriochlorophyll *a* (BChl *a*) and carotenoid binding sites in the LH1 complexes surrounded by these two different surfactant molecules. Polarizabilty change ($\Delta\boldsymbol{\alpha}$) and dipole moment change ($\Delta\boldsymbol{\mu}$) upon photoexcitation were determined for the BChl *a* Q_y band. Both of these parameters show smaller values in the presence of LDAO than in Triton X-100. This indicates that polar detergent molecules, like LDAO, affect the electrostatic environment around BChl *a*, and modify the nonlinear optical parameters ($\Delta\boldsymbol{\alpha}$ and $\Delta\boldsymbol{\mu}$ values). The electrostatic field around the BChl *a* binding site, which is generated by the presence of LDAO, was determined to be $|\mathbf{E}_L| = \sim 3.9 \times 10^5$ [V/cm]. Interestingly, this kind of electrostatic effect was not observed for the carotenoid-binding site. The present study demonstrates a unique electrostatic interaction between the polar detergent molecules surrounding the LH1 complex and the Q_y absorption band of BChl *a* that is bound to the LH1 complex.

Keywords Bacteriochlorophyll · Carotenoid · LH1 complex · Non-polar detergent · Polar detergent · Purple photosynthetic bacteria · Stark spectroscopy

Abbreviations

BChl *a*	Bacteriochlorophyll *a*
LDAO	*N*,*N*-lauryl dimethyl aminooxide
LH1	Light-harvesting 1 complex
RC	Reaction center
Rs. rubrum S1	*Rhodospirillum rubrum* strain S1

Introduction

The LH1 complexes of purple photosynthetic bacteria harvest solar energy and transfer the captured energy to reaction centers. They are embedded in photosynthetic membranes (lipid-bilayer system). These pigment–protein complexes are, therefore, always under the influence of potential fields formed by surrounding molecules (e.g., polar and non-polar lipid molecules, ionic small molecules, etc.). It is interesting to ask the question how such electrostatic potentials might affect the physical properties of the LH1 complexes, especially the pigment molecules bound to these complexes and, thereby, their physiological functions. So far, a little attention has been paid to this intriguing question; probing the electrostatic interaction inside the pigment–protein complexes is not straightforward. However, recent advances in Stark spectroscopy by

K. Nakagawa · M. Nango
Department of Applied Chemistry, Graduate School of Engineering, Nagoya Institute of Technology, Gokiso-cho, Nagoya 466-8555, Japan

S. Suzuki · R. Fujii · H. Hashimoto (✉)
Department of Physics, Graduate School of Science, Osaka City University, 3-3-138 Sugimoto, Sumiyoshi-ku, Osaka 558-8585, Japan
e-mail: hassy@sci.osaka-cu.ac.jp

A. T. Gardiner · R. J. Cogdell
Glasgow Biomedical Research Centre, Institute of Biomedical and Life Sciences, University of Glasgow, 120 University Place, Glasgow 8QQ, Scotland, UK

our group have made it possible to quantitatively probe these kinds of interactions (Yanagi et al. 2004, 2005).

Stark spectroscopy probes how an absorbance change is induced by externally applied electric fields. Electrostatic potentials generated by surrounding molecules affect the magnitude and direction of the induced polarizabilty change ($\Delta\boldsymbol{\alpha}$) and the static dipole moment change ($\Delta\boldsymbol{\mu}$) upon photoexcitation of the pigment molecules bound to the LH1 complexes, in the presence of an applied electric field. Using Stark spectroscopy we can determine these two optical parameters. Therefore, if we compare these parameters for LH1 complexes in different electrostatic environments, we can determine how the potential field generated by the surfactant molecules affects the physical properties of pigment molecules bound to the LH1 complexes. This approach assumes that there are no structural changes induced by the detergents. Stark spectroscopy is a well-established technique, and its physical interpretation is well worked out. Hence, it can be used reliably for quantitative analyses, such as those described below, where the Stark spectral data can be correlated with the still restricted structural information that is currently available for the LH1 complexes (Bahatyrova et al. 2004; Fotiadis et al. 2004; Jamieson et al. 2002; Karrasch et al. 1995; Roszak et al. 2003).

In this study, we have used Stark spectroscopy to investigate how two different detergents affect the electrostatic environment of the pigments in purified LH1 complexes from the purple photosynthetic bacterium, *Rhodospirillum* (*Rs.*) *rubrum* strain S1.

Materials and methods

Growth of the cells of *Rs. rubrum* S1 and preparation of chromatophores

Cells of *Rs. rubrum* strain S1 were grown anaerobically in the light in C-succinate media (modified from Cohen-Bazire et al. 1957) at 29°C. Continuous illumination was provided by 100 W tungsten–halogen lamps. The cells were harvested by centrifugation (18,800g × 10 min at 4°C), resuspended in 20 mM Tris–HCl buffer (pH 8.0), and stored in a freezer (–20°C) until use. Chromatophores were prepared, as described by Cogdell and Crofts (1978). Briefly, the cells were homogenized in 20 mM Tris–HCl buffer (pH 8.0) and a small amount of DNase and $MgCl_2$ were added. The cells were broken by two passages through a French press (140 MPa). Unbroken cells and cell-wall materials were removed by centrifugation (27,000g × 20 min at 4°C), and then the chromatophores were pelleted by ultracentrifugation (250,000g × 60 min at 4°C).

Preparation of LH1 complexes from *Rs. rubrum* S1

The LH1 complexes of *Rs. rubrum* S1 were prepared by a slight modification of the method of Picorel et al. (1983). Chromatophores of *Rs. rubrum* S1 were homogenized with 50 mM potassium phosphate buffer (pH 7.0), and then solubilized with the same buffer containing 0.5% LDAO as the detergent. This protocol releases the RCs from the RC-LH1 complexes. The solution after solubilization was subjected to ultracentrifugation (105,000g × 90 min at 4°C). The resulting pellet thus obtained was homogenized in 50 mM phosphate buffer (pH 7.0), and adjusted to an OD_{880} = 28. Then the solution was solubilized by the addition of 0.4% LDAO. This solubilized material was subjected to ultracentrifugation (105,000g × 90 min at 4°C), and the supernatant containing the major fraction of the LH1 complexes was collected. This LH1 solution was dialyzed against 50 mM Tris–HCl (pH 8.0) buffer for 3 days at 4°C. After the dialysis, the LH1 fraction was purified using a DE52 ion-exchange column. The DE52 column was equilibrated with 50 mM Tris–HCl (pH 8.0) buffer, containing 0.1% Triton X-100. The LH1 was purified by a step-gradient using the same buffer containing 25–250 mM NaCl. After purification NaCl was removed by dialysis, and the concentration of Triton X-100 in the LH1 solution was diluted to 0.025%.

The LDAO was re-added to some of the purified LH1 complexes by detergent exchange on a DE52 column, using 50 mM Tris–HCl (pH 8.0) buffer containing 0.08%. After washing the Triton X-100 away, the LH1 complexes were eluted by the addition of NaCl, dialyzed, and then diluted to give a final LDAO concentration of 0.025%.

All purification protocols were performed at 4°C and in the dark.

Spectroscopic analysis

Absorption and circular dichroism (CD) spectra were recorded, respectively, on JASCO V-530 UV-vis and JASCO J-720 CD spectrophotometers using a 1-cm optical path-length quartz cuvette. For the CD measurements, the absorbance of the LH1 complexes at the peak of the Q_y transition of BChl *a* was adjusted to an OD_{880} = 1.0. Fluorescence excitation spectra were recorded at 900 nm using a JASCO FP-6600 spectrofluorometer; the absorbance of the LH complexes was adjusted to an OD_{880} = 0.1. The singlet–singlet energy transfer efficiency from carotenoid to BChl *a* in the LH1 complexes was determined by comparing the area under the curves in the carotenoid region of the absorption and the fluorescence excitation spectra. For this comparison, the fractional absorbance (1—transmittance) was used. The absorption and fluorescence excitation spectra were

normalized at the Soret absorption band of BChl *a*. All these spectral measurements were performed at 4°C.

Sample cells for use in the Stark spectroscopic measurements were prepared, as previously reported (Yanagi et al. 2004, 2005). The LH1 complexes surrounded with surfactant molecules were uniformly dispersed in a PVA polymer, and were cast to form a film on the top of gold electrodes that are separated by 35–60 μm. Stark spectra were recorded using a home-built set up, the detail of which has already been reported (Yanagi et al. 2004, 2005). A sinusoidal electric field of 40 kV/cm was applied externally to the electrodes of the Stark cell with the frequency of $f = 500$ Hz. The small absorbance changes induced by this applied electric field were amplified using a dual phase lock-in amplifier (NF, 5610B). The second harmonic component ($2f$ component) of the electric-field-induced absorbance changes was selectively amplified.

Theory underlying Stark spectroscopy (Liptay equation)

The Stark effect, viz. the spectral changes induced by the application of an external electric field reflect the well-known Stark effect, is a third-order nonlinear optical effect; its theoretical background has been developed by Liptay (1974). The basic mathematical formalism (so-called Liptay equation) has been derived based on a second-order perturbation theory by taking the magnitude of the electric field as a perturbation.

Sample molecules (in the present case these are LH1 complexes surrounded by surfactants) were isotropically dispersed and immobilized in a polymer matrix. When they have a single absorption band, and the energy-shift (Stark shift) induced by the applied electric field is considerably smaller than the width of absorption band, the induced absorbance change ΔA in the Stark spectra can be described by the following formulae. In these equations the angle between the electric vector of incident radiation and the applied electric field is set to be $\chi = 54.7°$ (the magic angle configuration).

$$\Delta A(v) = \left[A_\chi \cdot A(v) + B_\chi \cdot \frac{v}{15hc} \frac{d\left(A(v)/v\right)}{dv} + C_\chi \cdot \frac{v}{30h^2c^2} \frac{d^2(A(v)/v)}{dv^2} \right] \cdot \mathbf{E}_{\text{int}}^2 \quad (1)$$

$$A_\chi = \frac{1}{3} \frac{1}{|\mathbf{M}|^2} \sum_{ij} \left(X_{ii} X_{jj} + M_i Y_{ijj} \right) \quad (2)$$

$$B_\chi = 5 \left\{ \frac{1}{2} \mathrm{Tr}(\Delta\boldsymbol{\alpha}) + \frac{2}{|\mathbf{M}|^2} \left(\sum_{ij} M_i X_{ij} \right) \cdot \Delta\boldsymbol{\mu} \right\} \quad (3)$$

$$C_\chi = 5|\Delta\boldsymbol{\mu}|^2 \quad (4)$$

Here v is the frequency of incident light, h is the Planck constant, c is the velocity of light, and $\mathbf{E}_{\text{int}}$ is the internal electric field. $\mathbf{E}_{\text{int}}$ can be expressed as $\mathbf{E}_{\text{int}} = f \cdot \mathbf{E}_{\text{a}}$, where $\mathbf{E}_{\text{a}}$ is the externally applied electric field and f is the Lorentz local-field correction factor. $\mathbf{M}$ is optical transition dipole moment. X and Y are its polarizabilty and hyperpolarizabilty, respectively. $\Delta\boldsymbol{\alpha}$ and $\Delta\boldsymbol{\mu}$ are the changes of polarizability and static dipole moment of this transition, respectively. As can be seen in Eq. (1), $\Delta A(v)$ can be represented as the sum of the zero-th, first, and second derivative of the original absorption spectrum $A(v)$.

In this study, the magnitude of the coefficient A_χ is negligibly small compared to that of B_χ or C_χ and takes negative values. Assuming that X can be neglected, A_χ and B_χ can be simplified as follows.

$$A_\chi \approx \frac{1}{3} \frac{1}{|\mathbf{M}|^2} \sum_{ij} \left(M_i Y_{ijj} \right) = \frac{1}{3} D \quad B_\chi \approx \frac{5}{2} \mathrm{Tr}(\Delta\boldsymbol{\alpha}) \quad (5)$$

By fitting Eq. (1) to the experimentally observed Stark spectra, we can determine $\mathrm{Tr}(\Delta\boldsymbol{\alpha})$ and $|\Delta\boldsymbol{\mu}|$. These two parameters are important nonlinear optical constants that reflect the physical properties of the pigment molecules in the LH1 complexes.

Results

In this study, the effect of two different detergents, LDAO and Triton X-100, on the spectroscopic properties of LH1 complexes from *Rs. rubrum* strain S1 have been investigated. For simplicity, they are called the LDAO preparation and the Triton preparation.

Figure 1 compares the absorption spectra of these two preparations. Both spectra show the well-known features of BChl *a* with absorption bands at 376 nm (Soret band), 589 nm (Q_x band), and about 880 nm (Q_y band). The absorption bands observed at 485, 514, and 549 nm in both preparations are due to the $S_0 \rightarrow S_2$ transitions of the carotenoids, and they correspond to the vibrational progression inherent to the $S_0 \rightarrow S_2$ transition. These absorption spectra agree well with those reported previously for LH1 complexes from *Rs. rubrum* S1 (Akahane et al. 2004; Fieder et al. 2004; Picorel et al. 1983). However, close inspection shows that there is a slight difference

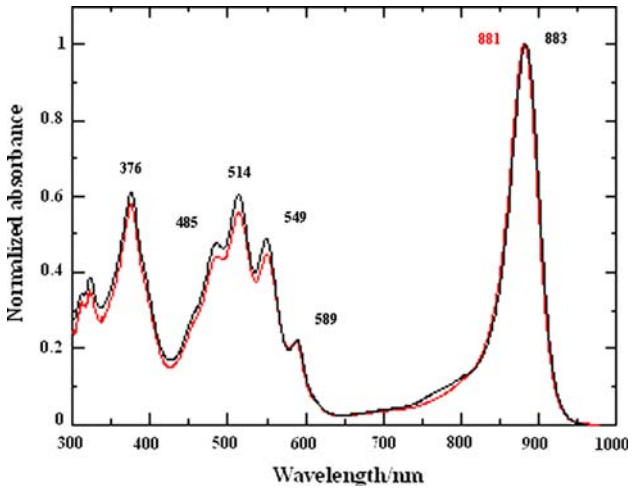

Fig. 1 Normalized (Qy-band) absorption spectra of LH1 complexes isolated from *Rs. rubrum* S1 in 0.025% LDAO (solid red-line) and in 0.025% Triton X-100 (solid black line). Both these samples were dissolved in 50 mM Tris–HCl (pH 8.0) buffer solutions. Spectra were recorded at 4°C

in the wavelength maximum of the Q_y band in the two preparations. The LDAO preparation has a Q_y maximum at 883 nm, while the Triton preparation has a peak at 881 nm. This 2 nm difference is small but very reproducible.

Figure 2 compares the CD spectra of the LDAO and the Triton preparations. In the BChl *a* Soret and Q_x regions, and the carotenoid absorptions, the wavelengths of the spectral features are identical. However, small, but reproducible, differences can again be seen in the Q_y absorption region. In both preparations similar types of spectral splitting are observed in the Q_y region, but the peak wavelengths differ slightly between the LDAO preparation

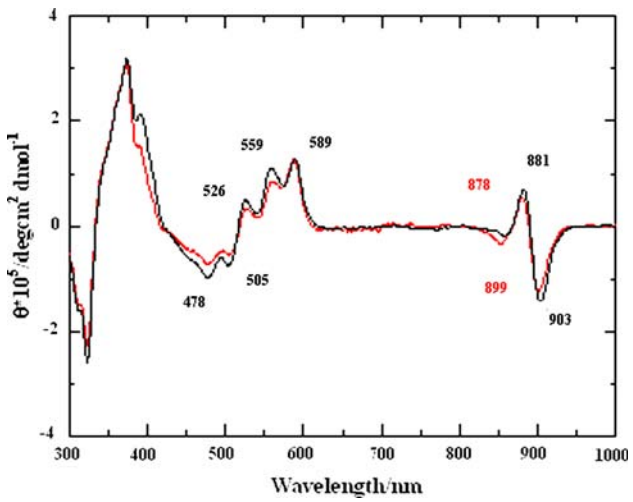

Fig. 2 Circular dichroism (CD) spectra of LH1 complexes isolated from *Rs. rubrum* S1 in 0.025% LDAO (solid red-line) and in 0.025% Triton X-100 (solid black line). Both these samples were dissolved in 50 mM Tris–HCl (pH 8.0) buffer solutions. Spectra were recorded at 4°C. They were normalized to equal absorption of the Q_y-band

(881 and 903 nm) and the Triton preparation (878 and 899 nm). Like in absorption, the LDAO preparation shows a 3–4 nm longer wavelength shift than the Triton preparation.

Figure 3 compares normalized Stark spectra of the LDAO and Triton preparations. Here, the Stark spectra were normalized against the intensity of the applied electric field and the concentration of the samples. Hence it is possible to compare directly the magnitudes of these two spectra. In the carotenoid and Q_x absorption regions (400–650 nm), the LDAO and Triton preparations show very similar spectral features. In contrast, the two spectra show pronounced differences in the Q_y absorption region (700–1000 nm). In this regard Stark spectroscopy provides a very sensitive method with which to probe subtle changes in the local environment of chromophores bound to proteins. Table 1 shows the calculated magnitudes of the nonlinear optical parameters of both the carotenoid and BChl *a* Q_y absorption bands determined by Stark spectroscopy. $Tr(\Delta\alpha)$ and $|\Delta\mu|$ values of the carotenoid absorption bands are essentially the same in both the LDAO and Triton preparations. However, for the BChl *a* Q_y absorption band both these parameters are smaller in the LDAO preparation than in the Triton preparation. These results clearly show that the Q_y absorption band of BChl *a* is influenced by the electrostatic field generated by the polar detergent molecule LDAO.

Finally, the energy transfer efficiency from carotenoid to BChl *a* was determined by fluorescence-excitation spectroscopy. Both the LDAO and Triton preparations showed a similar efficiency of 28%.

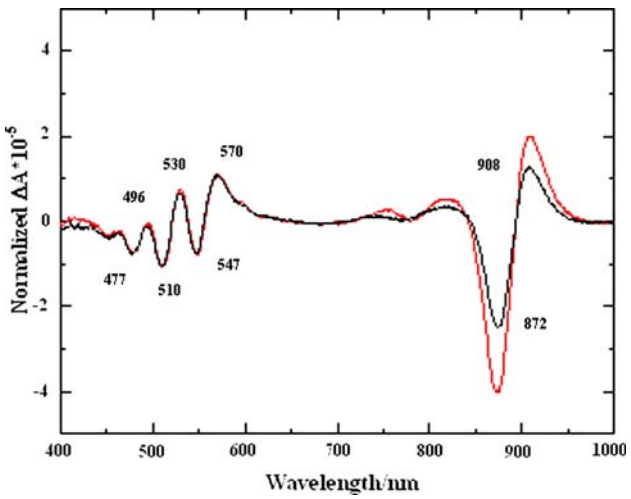

Fig. 3 Normalized Stark spectra of LH1 complexes isolated from *Rs. rubrum* S1 in 0.025% LDAO (solid red-line) and in 0.025% Triton X-100 (solid black line). The normalization was performed against the intensity of applied electric field as well as the concentration of the samples. Both samples were dispersed and immobilized isotropically in PVA films. Spectra were recorded at room temperature

Table 1 Nonlinear optical parameters (Tr($\Delta\alpha$) and $|\Delta\mu|$) of carotenoid and BChl *a* Q_y absorption bands determined by Stark spectroscopy of LH1 complexes isolated from *Rs. rubrum* S1 in 0.025% Triton X-100 and in 0.025% LDAO

Purified complete LH1 complex from *Rs. Rubrum* S1	Carotenoid		BChl *a* (Q_y)	
	Tr($\Delta\alpha$) (Å^3/f^2)	$\|\Delta\mu\|$ (D/f)	Tr($\Delta\alpha$) (Å^3/f^2)	$\|\Delta\mu\|$ (D/f)
In 0.025% Triton X-100	1400 ± 100	7.2 ± 0.2	390 ± 30	5.5 ± 0.1
In 0.025% LDAO	1400 ± 100	7.1 ± 0.2	300 ± 20	4.2 ± 0.1

Discussion

In this study, we have quantitatively evaluated the electrostatic effect generated by surfactant molecules on the carotenoid and BChl *a* Q_y absorption bands of purified LH1 complexes. The results of Stark spectroscopy show that the polar detergent molecules (LDAO) have a clear electrostatic interaction with the Q_y absorption band of BChl *a*. In the following section we discuss a possible physical origin of this specific interaction.

The LH1 complex of *Rs. rubrum* is composed of 16 subunits of a pair of LH1-α and LH1-β polypeptides and has a circular ring structure (Jamieson et al. 2002; Karrasch et al. 1995). Each subunit has two BChl *a* and one carotenoid molecules. In other words, 32 BChl *a* molecules are arranged circularly with 16-fold rotation symmetry. In this case, the Q_y absorption band BChl *a* should have exciton splitting and form an exciton-band system with 18 sublevels. According to symmetry considerations, and neglecting any deviation from a circular arrangement, most of these are doubly degenerate, as shown in Fig. 4. Recent high-resolution atomic-force microscopy studies have shown that the structure of LH1 complexes can be rather flexible, and sometimes appear as ellipses or C shaped structures (Bahatyrova et al. 2004). In these cases the degeneracy of the exciton bands is relaxed and the 18 sublevels independently contribute to form the Q_y absorption band (see Fig. 4) (Katelaars et al. 2002; Leupold et al. 2000). In either case, of circular or non-circular structures for LH1, the absorption from the ground state to the lowest and the third lowest exciton sub-levels of Q_y band are initially one-photon forbidden. In the latter case, however, these transitions become partially allowed and the magnitude of transition dipole moment depends on the degree of deformation.

Therefore, the transition from the ground-state to the second lowest exciton sub-level (ε_2 shown in Fig. 4) is responsible for the Q_y absorption band observed around 880 nm in Fig. 1. This means that it is possible to concentrate on the four level system composed of groundstate (ε_0), the lowest exciton sub-level (ε_1), ε_2, and the third lowest exciton sub-level (ε_3) in order to understand the

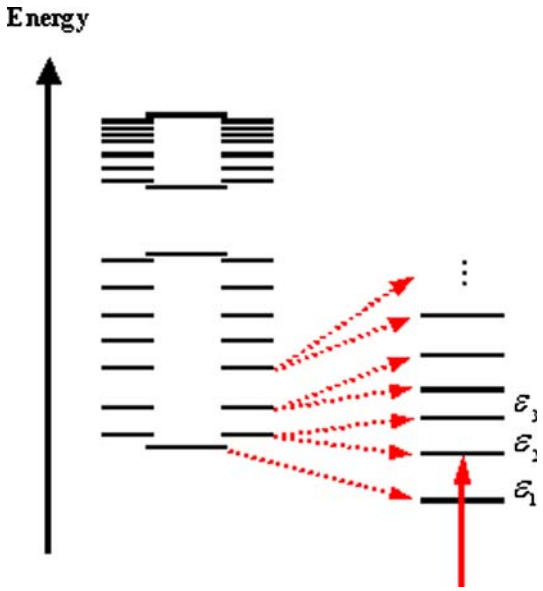

Fig. 4 Schematic description of excitonic sub-levels of dimeric BChl *a* in the LH1 complex circularly arranged with 16-fold rotation symmetry (left-hand side), and in a complex with broken symmetry (right-hand side). ε_2, and ε_3 denote the energies of the lowest, second lowest, and third lowest exciton sub-levels, respectively. The vertical solid red arrow in the right-hand side diagram shows the one-photon allowed transition from the ground state

results presented above. We can postulate that the polar detergent LDAO induces an electric field $\mathbf{E}_L$ around BChl *a* that has a specific electrostatic interaction with the Q_y band. Therefore, we can apply second order perturbation theory in order to derive the wavefunctions and energy levels of each exciton sub-level of Q_y band of BChl *a* bound to the LH1 complex in the LDAO preparation. For this calculation, the interaction energy of $-\boldsymbol{\mu} \cdot \mathbf{E}_L$ was taken as a perturbation. Here, $\boldsymbol{\mu}$ shows the transition dipole moment of the transitions from the groundstate to each exciton sub-level of the Q_y band in the unperturbed system (the LH1 complexes in Triton preparation). We denote the unperturbed wavefunctions that are associated with the ε_1, ε_2, and ε_3 exciton sub-levels in Triton preparation, respectively, as $|1\rangle$, $|2\rangle$, and $|3\rangle$. Then the perturbed wavefunctions ($|1^{\mathbf{E}_L}\rangle$,$|2^{\mathbf{E}_L}\rangle$, $|3^{\mathbf{E}_L}\rangle$) and energy levels ($\varepsilon_1^{\mathbf{E}_L}$, $\varepsilon_2^{\mathbf{E}_L}$, and $\varepsilon_3^{\mathbf{E}_L}$) can be derived as follows.

$$|1^{\mathbf{E}_L}\rangle \approx |1\rangle + |2\rangle \frac{\boldsymbol{\mu}_{12}\cdot\mathbf{E}_L}{\varepsilon_1-\varepsilon_2} + |3\rangle \frac{\boldsymbol{\mu}_{31}\cdot\mathbf{E}_L}{\varepsilon_3-\varepsilon_1} \quad (6)$$

$$|2^{\mathbf{E}_L}\rangle \approx |2\rangle - |1\rangle \frac{\boldsymbol{\mu}_{21}\cdot\mathbf{E}_L}{\varepsilon_3-\varepsilon_1} + |3\rangle \frac{\boldsymbol{\mu}_{23}\cdot\mathbf{E}_L}{\varepsilon_3-\varepsilon_2} \quad (7)$$

$$|3^{\mathbf{E}_L}\rangle \approx |3\rangle - |1\rangle \frac{\boldsymbol{\mu}_{31}\cdot\mathbf{E}_L}{\varepsilon_3-\varepsilon_1} - |3\rangle \frac{\boldsymbol{\mu}_{32}\cdot\mathbf{E}_L}{\varepsilon_3-\varepsilon_2} \quad (8)$$

$$\varepsilon_1^{E_L} \approx \varepsilon_1 - \Delta\boldsymbol{\mu}_{11}\cdot\mathbf{E}_L \quad (9)$$

$$\varepsilon_2^{E_L} \approx \varepsilon_2 - \Delta\boldsymbol{\mu}_{22}\cdot\mathbf{E}_L \quad (10)$$

$$\varepsilon_3^{E_L} \approx \varepsilon_3 - \Delta\boldsymbol{\mu}_{33}\cdot\mathbf{E}_L \quad (11)$$

Equations (6)–(8) illustrate how the transition intensity may change under the perturbation of $\mathbf{E}_L$. By calculating the matrix element of one-photon transitions from the ground state to each of the perturbed exciton sub-levels, it is possible to show that the forbidden nature of the transitions to the $|1\rangle$ and $|3\rangle$ states from the ground state are relaxed to some extent. On the other hand, the transition intensity to the $|2\rangle$ state is decreased. This corresponds to an intensity borrowing process under the influence of the perturbation. Importantly, Eq. (10) describes the background principle that can explain why the Q_y absorption band of LDAO preparation shows 2-nm longer wavelength maximum from that of the Triton preparation. Since $\Delta\boldsymbol{\mu}_{22}$ has already been determined by Stark spectroscopy (see $|\Delta\boldsymbol{\mu}|$ of BChl *a* Q_y band in Table 1), we can determine the magnitude of $|\mathbf{E}_L|$ to be 3.9×10^5 [V/cm] using Eq. (10). Here, we have adopted the value of $f = 1.4$ as a local-field correction factor (Nagae et al. 1994).

$\mathrm{Tr}(\Delta\boldsymbol{\alpha})$ can be expressed as follows based on the same four-level scheme.

$$\mathrm{Tr}(\Delta\boldsymbol{\alpha}) \approx 2\left(\frac{\boldsymbol{\mu}_{23}\boldsymbol{\mu}_{32}}{\varepsilon_3-\varepsilon_2} - \frac{\boldsymbol{\mu}_{12}\boldsymbol{\mu}_{21}}{\varepsilon_2-\varepsilon_1}\right) \quad (12)$$

Here, subscripts 1, 2, and 3 correspond to the $|1\rangle$, $|2\rangle$, and $|3\rangle$ states, respectively. The results of Stark spectroscopy show that BChl *a* Q_y band in the LDAO preparation has smaller value of $\mathrm{Tr}(\Delta\boldsymbol{\alpha})$ than that in the Triton preparation. According to Eq. (12), this observation indicates that the second term in right-hand side of Eq. (12) has the stronger contribution to $\mathrm{Tr}(\Delta\boldsymbol{\alpha})$ under the influence of the perturbation ($\mathbf{E}_L$) by LDAO. This can either be caused by a reduced energy gap ($\varepsilon_2 - \varepsilon_1$), or by an increase of the transition dipole moment ($\boldsymbol{\mu}_{12}\boldsymbol{\mu}_{21}$).

On the basis of the theoretical discussion presented above the spectroscopic results can be summarized as follows. (1) All the relevant excitonic sub-levels ($|1\rangle$,$|2\rangle$, and $|3\rangle$) lower their energy (see Eqs. (9)–(11)). (2) The transition intensity from the ground-state to the $|1\rangle$ state, which is one-photon forbidden in the unperturbed condition, is increased, while that to the $|2\rangle$ state is decreased. (3) The energy gap ($\varepsilon_2 - \varepsilon_1$) between the $|1\rangle$ and $|2\rangle$ states decreases (see Ketelaars et al. 2002, for supportive information). The combination of these two effects explains the shift by 2 nm of the wavelength maximum of the BChl *a* Q_y absorption band of the LDAO preparation in comparison to that of the Triton preparation. The third effect explains the decrease of the magnitude of the $\mathrm{Tr}(\Delta\boldsymbol{\alpha})$ of the BChl *a* Q_y absorption band in the LDAO preparation. The fact that the energy (stabilization) of the $|1\rangle$, $|2\rangle$, and $|3\rangle$ states decreases in the presence of $\mathbf{E}_L$ indicates that the direction of $\Delta\boldsymbol{\alpha}$ of the BChl *a* Q_y absorption band is antiparallel to the direction of $\mathbf{E}_L$.

The results demonstrate the presence of a specific electrostatic interactions between the polar detergent molecules and the Q_y absorption band of BChl *a* in the LH1 complex. This interaction can be seen only in this absorption band because of the direction of its transition dipole moment with respect to the direction of the local electrostatic field. One of the Soret bands is also y-polarized, and hence it is expected that the similar effect can also be seen in the Soret region. However, this spectral region is out of the detection limit of the present set-up of Stark spectroscopy, and it is not possible to discuss this issue. The efficiency of carotenoid to BChl *a* energy transfer (28%) does not change in these two preparations. This is consistent with previous findings. The main carotenoid that is included in the present preparations of LH1 is spirilloxanthin, which has 13 conjugated C = C bonds. Based on studies using sub-picosecond transient absorption spectroscopy (Akahane et al. 2004; Gradinaru et al. 2001) it has been reported that the main channel of the energy transfer from spirilloxanthin to BChl *a* utilizes the S_2 ($1^1B_u^+$) state of spirilloxanthin and the Q_x state of BChl *a*. The present study shows that polar detergent molecules can perturb mainly the electrostatic environment of the BChl *a* Q_y absorption band. Since this singlet–singlet energy-transfer goes via the Q_x state, it is expected that the efficiency of this reaction is not changed by the presence of LDAO.

In conclusion, in this study, we have demonstrated that the Stark spectroscopy is a powerful technique to probe the effects on the local electrostatic field caused by the presence of polar detergent micelles surrounding the LH1 complex. The LDAO molecules induce electric field of $|\mathbf{E}_L| \approx 3.9 \times 10^5$ [V/cm] and this affects mainly the electronic properties of the Q_y absorption band of BChl *a*. In the native photosynthetic membranes, proteins are surrounded by lipid molecules and the composition of these lipid molecules may change depending on the species of

bacteria (Benning 1998). Also, the lipids around the complexes may differ from the bulk lipids (Kwa et al. 2007). Therefore, the electrostatic environment formed by these lipid molecules may change around the pigment–protein complexes depending on how many polar lipid molecules surround that protein. It is not clear at this stage whether such differences in the electrostatic environment can affect the physiological functions the pigment–protein complexes. However, Stark spectroscopy provides a sensitive tool with which to investigate this issue.

Acknowledgements This work was supported by the Grant-in-aid from the Japanese Ministry of Education, Culture, Sports, Science, and Technology (Grants No. 17204026, No. 17654083). Hideki Hashimoto, Ritsuko Fujii, Mamoru Nango, Alastair T. Gardiner and Richard J. Cogdell thank for the financial support from SICP/JST. Hideki Hashimoto also acknowledges for the support from PRESTO/JST. Richard J. Cogdell and Alastair T. Gardiner thank for the financial support from BBSRC.

References

Akahane J, Rondonuwu FS, Fiedor L, Watanabe Y, Koyama Y (2004) Dependence of singlet-energy transfer on the conjugation length of carotenoids reconstituted into the LH1 complex from *Rhodospirillum rubrum* G9. Chem Phys Lett 393:184–191

Bahatyrova S, Frese RN, van der Werf KO, Otto C, Hunter CN, Olsen JD (2004) Flexibility and size heterogeneity of the LH1 light harvesting complex revealed by atomic force microscopy: functional significance for bacterial photosynthesis. Biol Chem 279:21327–21333

Benning C (1998) Membrane lipids in anoxygenic photosynthetic bacteria. In: Siegenthaler P-A, Murata N (eds) Lipids in photosynthesis: structure, function, and genetics, vol 6. Kluwer Academic Publishers, Dordrecht, The Netherlands, pp 83–101

Cogdell RJ, Crofts AR (1978) Analysis of the pigment content of an antenna pigment-protein complex from three strains of *Rhodopseudomonas sphaeroides*. Biochim Biophys Acta 502:409–416

Cohen-bazire G, Sistrom WR, Stanier RY (1957) Kinetic studies of pigment synthesis by non-sulfur purple bacteria. J Cell Comp Physiol 49:25–68

Fiedor L, Akahane J, Koyama Y (2004) Carotenoid-induced cooperative formation of bacterial photosynthetic LH1 complex. Biochemistry 43:16487–16496

Fotiadis D, Qian P, Philippsen A, Bullough PA, Engel A, Hunter CN (2004) Structural analysis of the reaction center light-harvesting complex I photosynthetic core complex of *Rhodospirillum rubrum* using atomic force microscopy. J Biol Chem 279:2063–2068

Gradinaru CC, Kennis JTM, Papagiannakis E, van Stokkum IHM, Cogdell RJ, Fleming GR, Niederman RA, van Grondelle R (2001) An unusual pathway of excitation energy deactivation in carotenoids: singlet-to-triplet conversion on an ultrafast timescale in a photosynthetic antenna. Proc Natl Acad Sci USA 98:2364–2369

Jamieson SJ, Wang P, Qian P, Kirkland JY, Conroy MJ, Hunter CN, Bullough PA (2002) Projection structure of the photosynthetic reaction centre-antenna complex of *Rhodospirillum rubrum* at 8.5 Å resolution. EMBO J 21:3927–3935

Karrasch S, Bulloughl PA, Ghosh R (1995) The 8.5 Å projection map of the light-harvesting complex I from *Rhodospirillum rubrum* reveals a ring composed of 16 subunits. EMBO J 14:631–638

Ketelaars M, Hofmann C, Köhler J, Howard TD, Cogdell RJ, Schmidt J, Aartsma TJ (2002) Spectroscopy on individual light-harvesting 1 complexes of *Rhodopseudomonas acidophila*. Biophys J 83:1701–1715

Kwa LG, Wegmann D, Wanner G, Braun P (2007) Mutation of a single residue, glutamate β10, alters protein-lipid interactions of light harvesting complex II. Presentation at PS2007 Satellite Meeting of Light-Harvesting Systems Workshop, 19th–22nd July in Drymen, Scotland, UK

Leupold D, Voigt B, Beenken W, Stiel H (2000) Pigment-protein architecture in the light-harvesting antenna complexes of purple bacteria: does the crystal structure reflect the native pigment-protein arrangement? FEBS Lett 480:73–78

Liptay W (1974) Dipole moments and polarizabilities of molecules in excited electronic states. In: Lin EC (ed) Excited states, vol 1. Academic Press, New York, USA, pp 129–229

Nagae H, Kuki M, Cogdell RJ, Koyama Y (1994) Shifts of the $1A_g^- \rightarrow 1B_u^+$ electronic absorption of carotenoids in nonpolar and polar solvents. J Chem Phys 101:6750–6765

Picorel R, Bélanger G, Gingras G (1983) Antenna holochrome B880 of *Rhodospirillum rubrum* S1: pigment, phospholipid, and polypeptide composition? Biochemistry 22:2491–2497

Roszak AW, Howard TD, Southall J, Gardiner AT, Law CJ, Isaacs NW, Cogdell RJ (2003) Crystal structure of the RC-LH1 complex from *Rhodopseudomonas palustris*. Science 302:1969–1972

Yanagi K, Hashimoto H, Gardiner AT, Cogdell RJ (2004) Stark spectroscopy on the LH2 complex from *Rhodobacter sphaeroides* strain G1C: frequency and temperature dependence. J Phys Chem B 108:10334–10339

Yanagi K, Shimizu M, Hashimoto H, Gardiner AT, Roszak AW, Cogdell RJ (2005) Local electrostatic field induced by the carotenoid bound to the reaction center of the purple photosynthetic bacterium *Rhodobacter sphaeroides*. J Phys Chem B 109:992–998